PHYSICAL REVIEW B **83**, 100501(R) (2011)

Upper critical field of the pressure-induced superconductor $EuFe_2As_2$

Nobuyuki Kurita,[1,2] Motoi Kimata,[1,2] Kota Kodama,[1,3] Atsushi Harada,[1] Megumi Tomita,[1] Hiroyuki S. Suzuki,[1] Takehiko Matsumoto,[1] Keizo Murata,[4] Shinya Uji,[1,2,3] and Taichi Terashima[1,2]
[1]*National Institute for Materials Science, Tsukuba, Ibaraki 305-0003, Japan*
[2]*JST, Transformative Research Project on Iron Pnictides (TRIP), Chiyoda, Tokyo 102-0075, Japan*
[3]*Graduate School of Pure and Applied Sciences, University of Tsukuba, Ibaraki 305-0003, Japan*
[4]*Division of Molecular Materials Science, Graduate School of Science, Osaka City University, Osaka 558-8585, Japan*
(Received 22 November 2010; revised manuscript received 19 January 2011; published 8 March 2011)

We have carried out high-field resistivity measurements up to 27 T in $EuFe_2As_2$ at $P = 2.5$ GPa, a virtually optimal pressure for the P-induced superconductivity, where $T_c = 30$ K. The $B_{c2}-T_c$ phase diagram has been constructed in a wide temperature range with a minimum temperature of 1.6 K ($\approx 0.05 \times T_c$), for both $B \parallel ab$ (B_{c2}^{ab}) and $B \parallel c$ (B_{c2}^{c}). The upper critical fields $B_{c2}^{ab}(0)$ and $B_{c2}^{c}(0)$, determined by the onset of resistive transitions, are 25 and 22 T, respectively, which are significantly smaller than those of other Fe-based superconductors with similar values of T_c. The small $B_{c2}(0)$ values and the $B_{c2}(T)$ curves with positive curvature around 20 K can be explained by a multiple pair-breaking model that includes the exchange field due to the magnetic Eu^{2+} moments. The anisotropy parameter, $\Gamma = B_{c2}^{ab}/B_{c2}^{c}$, in $EuFe_2As_2$ at low temperatures is comparable to that of other "122" Fe-based systems.

DOI: 10.1103/PhysRevB.83.100501 PACS number(s): 74.70.Xa, 74.25.Op, 74.25.Dw, 74.62.Fj

The discovery of superconductivity in LaFeAs(O,F) at $T_c = 26$ K[1] has inspired experimental and theoretical research on a group of FeAs-layered superconductors (SCs).[2] Basically, Fe-based high-T_c superconductivity[3–5] occurs when the antiferromagnetic (AF) order in the mother compounds is suppressed by means of carrier doping,[1] application of pressure (P),[6] or isovalent substitution.[7] As compared to other methods in studying such interplay between magnetism and superconductivity, pressure experiments have a significant advantage in that they are free from random impurity potentials that may distort the underlying physics of the low-lying energy states. Among the various crystal structures, tetragonal $ThCr_2Si_2$-type ("122") compounds have been investigated more intensively owing to the availability of highly pure stoichiometric single crystals. In particular, AFe_2As_2 ($A =$ Sr, Eu) exhibits P-induced bulk superconductivity with T_c of order 30 K.[6,8,9] In contrast, superconductivity under hydrostatic pressure is not exhibited by $CaFe_2As_2$,[10] and its occurrence in $BaFe_2As_2$ has not been established definitively.[8,11]

A fundamental characteristic of SCs is the upper critical field B_{c2}. B_{c2} has its roots in the breakdown of Cooper pairs; hence, the $B_{c2}-T_c$ phase diagram provides important insights into the pairing mechanism of high-T_c superconductivity. Thus far, to our knowledge, there have been no reports on B_{c2} for P-induced Fe-based SCs at low temperatures. This is mainly attributed to the difficulty in conducting high-pressure experiments on high-T_c SCs under a high field. In the case of $SrFe_2As_2$ ($T_c = 30$ K at 4.2 GPa), a field of 8 T brings about a small reduction in T_c (i.e., to 27 K) for $B \parallel ab$.[13] Assuming an orbitally limited case,[12] B_{c2} ($T = 0$ K) could exceed 60 T.[13] However, the low temperature region of the B_{c2} curve, where paramagnetic and/or multiband effects may play important roles,[14] merits investigation.

In the case of $EuFe_2As_2$ ($T_c = 30$ K at $\sim$2.5 GPa), B_{c2} is relatively small (i.e., $\sim$16 T between 5 and 10 K)[9] and hence can be traced down to very low temperatures. $EuFe_2As_2$ is unique in that the localized Eu^{2+} moments exhibit an AF order below 20 K[15–19] in addition to an AF order arising from the FeAs layers at $T_0 \sim 190$ K. T_N of the Eu^{2+} moments is insensitive to pressure, and the AF order occurs in the P-induced superconducting state as evidenced by magnetic and heat capacity measurements under high pressure.[9,20–22] Despite the AF order, which is produced by a weak interlayer interaction, the dominant interaction among the Eu^{2+} moments is the intralayer ferromagnetic (FM) interaction, and hence the FM alignment of the Eu^{2+} moments is easily achieved by the application of 1 $\sim$ 2 T even below T_N at ambient pressure as well as under high pressure.[9,18–20,23,24] Thus, $EuFe_2As_2$ provides an excellent opportunity where a long-standing issue of the interplay between superconductivity and magnetism can be studied in a high-T_c material using high-quality single crystals.

In this report, we present the $B_{c2}-T_c$ phase diagram of $EuFe_2As_2$ at a pressure of 2.5 GPa and minimum temperature of 1.6 K via high-field resistivity measurements up to 27 T, and discuss the origin of the distinctive B_{c2} curves.

Single crystals of $EuFe_2As_2$ were prepared via the Bridgman method from a stoichiometric mixture of the constituent elements. The samples analyzed in this study were obtained from the same batch (residual resistivity ratio $RRR = 7$) as that used in Refs. 9,21, and 23. The resistivity of two samples, denoted by #1 and #2, was simultaneously measured at $P = 2.5$ GPa via an ac four-probe method in a ^{4}He cryostat ($T \geqslant$ 1.6 K). Sample #1 (#2) was aligned with the ab plane (c axis) parallel to the longitudinal direction of a hybrid-type piston cylinder pressure cell[25] for $B \parallel ab$ ($\parallel c$) measurements. For both samples, the magnetic field was applied along the piston cylinder axis in a direction perpendicular to that of the current. To generate hydrostatic pressure, Daphne 7474 (Idemitsu Kosan) oil, which remains in the liquid state up to 3.7 GPa at room temperature,[26] was used as the pressure-transmitting medium. The samples were gradually cooled at an average rate of 0.5 K/min. The pressure was calibrated at 4.2 K by

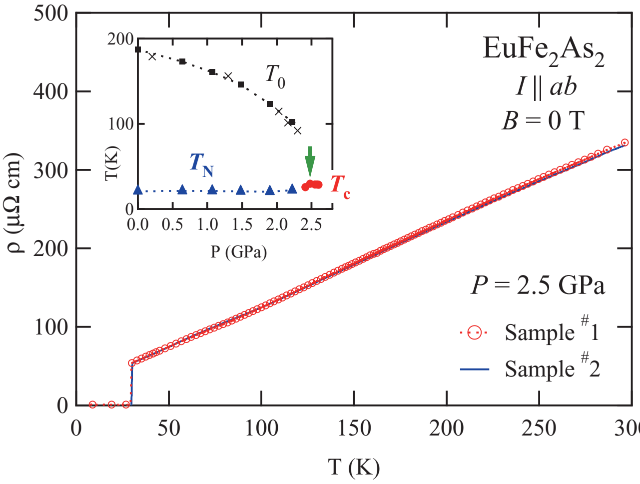

FIG. 1. (Color online) ρ vs T for $EuFe_2As_2$ at $P = 2.5$ GPa for samples #1 and #2 in the absence of applied field. The direction of current I is $I \parallel ab$. The inset illustrates the $T-P$ phase diagram of $EuFe_2As_2$.[29] T_0 and T_N denote the temperatures of the AF order arising from the FeAs layers and localized Eu^{2+} moments, respectively. The solid circles denote T_c determined under the criterion $\rho = 0$. The crosses denote the values obtained from Ref. 20.

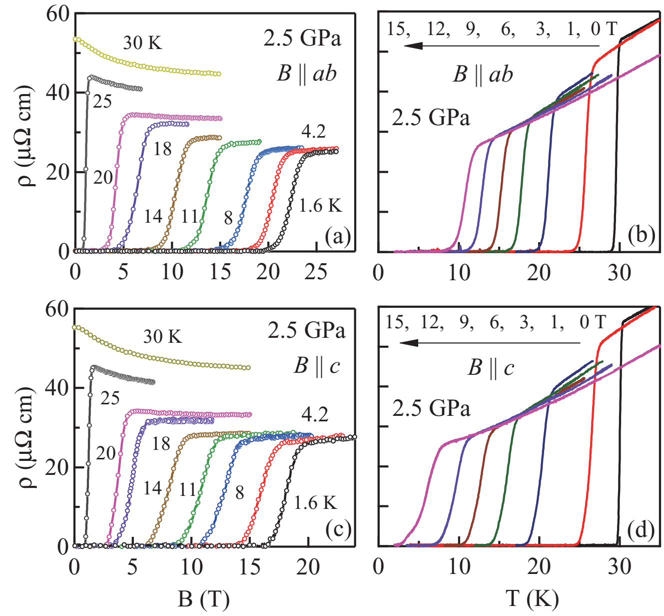

FIG. 2. (Color online) (a) ρ vs B and (b) ρ vs T for $B \parallel ab$ (sample #1) and (c) ρ vs B and (d) ρ vs T for $B \parallel c$ (sample #2) in $EuFe_2As_2$ at $P = 2.5$ GPa.

the resistance change of a Manganin wire.[9] Magnetic fields up to 27 T were produced by a water-cooled resistive magnet installed at the Tsukuba Magnet Laboratory, National Institute for Materials Science. A 17-T superconducting magnet was used for preliminary resistivity studies. In this study, the magnetic field B denotes an externally applied field, and the magnetization within a sample (up to ∼0.9 T[23]) is neglected.

Figure 1 shows the temperature dependence of the resistivity, $\rho(T)$, for the two samples, #1 and #2, at $P = 2.5$ GPa in the absence of an applied field. For both samples, ρ exhibits virtually T-linear dependence in the broad temperature range above T_c without any anomaly due to the AF order of the FeAs layers. This observation is consistent with the phase diagram shown in the inset:[20,29] $P = 2.5$ GPa is just above the critical pressure P_c, where $T_0 \to 0$, as indicated by the arrow. Similar $\rho \sim T$ behavior was also reported in several optimally doped Fe-based SCs.[27,28] However, the reason for such behavior is unclear. Both samples exhibit a sharp transition to zero resistivity at $T_c = 30$ K; the reentrant-like behavior as reported in Ref. 20 is not observed for either sample at this pressure. Our previous work[21] indicates that reentrant-like behavior may be observed for $P < P_c$ but not for $P > P_c$ (as long as P is not far from P_c) in our single crystals. Since both T_c and B_{c2} attain maximum values at $P \approx P_c$, followed by a monotonic decrease with increasing P,[29] B_{c2} determined at 2.5 GPa in this study is expected to be close to its maximum value.

Figures 2(a)–2(d) shows the resistivity of $EuFe_2As_2$ at 2.5 GPa as a function of B and T for the two orientations $B \parallel ab$ and $B \parallel c$. A magnetic field of 27 T is sufficient to recover the normal state at the minimum temperature, 1.6 K ($\approx 0.05 \times T_c$), for both orientations. Using the data in Figs. 2(a) and 2(b), the $B_{c2}-T_c$ phase diagram of $EuFe_2As_2$ is constructed for $B \parallel ab$ at 2.5 GPa, as shown in Fig. 3. Three sets—B_{c2}^{on} (onset), and B_{c2}^{x} ($x = 0$ and 50, x% of the normal state resistivity ρ_n)—are plotted, and their definitions are illustrated in the inset. The solid and open symbols are obtained from the $\rho(B)$ and $\rho(T)$ measurements, respectively. B_{c2}^{0} is consistent with the previous result (×) obtained from the ac-χ measurement for $B \parallel ab$.[9] Note that all the curves of B_{c2} for $B \parallel ab$ (B_{c2}^{ab}) obtained under different criteria exhibit qualitatively similar T dependence. The same is also true for B_{c2} for $B \parallel c$ (B_{c2}^{c}), as shown in Fig. 4(a). T_N at zero field is indicated by an arrow in Figs. 3 and 4. However, we note that, since the AF order of the Eu^{2+} moments is destroyed by an applied field of ∼1 T,[9] the B_{c2} curves for both $B \parallel ab$ and $B \parallel c$ are in the paramagnetic or field-induced FM state of the Eu^{2+} moments.

A distinctive feature, the concave (upward) curvature of B_{c2}^{ab} around 20 K, seems to be absent from other Fe-based SCs without localized magnetic ions. Therefore, it is likely related to the magnetic state of the Eu^{2+} moments. Similar concave $B_{c2}(T)$ curves have been reported in Chevrel-phase compounds such as (Eu,M)Mo_6S_8 (M = Sn,[30] La,[31] etc.) and $EuMo_6S_8$ under pressure.[32] In these systems, the conduction electrons are subjected to an exchange field B_J in addition to an applied field via AF coupling with the Eu^{2+} localized magnetic moments. Note that the concave curvature is an indication of the negative sign of B_J; B_J is antiparallel to the applied field.[32,33] Within a multiple pair-breaking picture, B_{c2} in the dirty limit of three-dimensional SCs with negative B_J can be expressed by[12,34]

$$\ln\frac{1}{t} = \left(\frac{1}{2}+\frac{i\lambda_{so}}{4\gamma}\right)\times\Psi\left(\frac{1}{2}+\frac{h+i\lambda_{so}/2+i\gamma}{2t}\right) + \left(\frac{1}{2}-\frac{i\lambda_{so}}{4\gamma}\right)\times\Psi\left(\frac{1}{2}+\frac{h+i\lambda_{so}/2-i\gamma}{2t}\right)-\Psi\left(\frac{1}{2}\right)$$
$$\gamma = \left[\alpha^2(h+h_J)^2-\lambda_{so}^2\right]^{\frac{1}{2}}, \quad (1)$$

where Ψ and λ_{so} are the digamma function and spin-orbit scattering parameter, respectively. The magnetic scattering

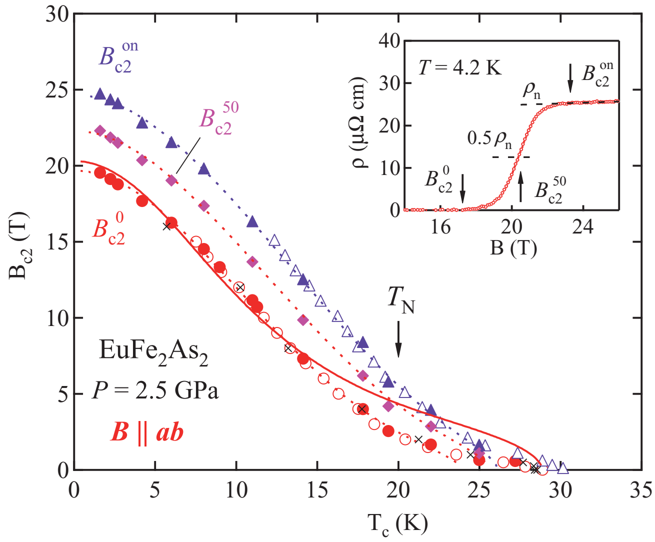

FIG. 3. (Color online) $B_{c2}-T_c$ phase diagram of $EuFe_2As_2$ for $B \parallel ab$ at 2.5 GPa. The values of B_{c2} are determined under three different criteria, as illustrated for $\rho(B)$ data at 4.2 K (inset). The solid or open symbols denote B_{c2} determined from $\rho(B)$ and $\rho(T)$ measurements, respectively. The solid and dashed curves are fits to Eq. (1). $\times$ denotes the previous B_{c2}^0 result deduced from an ac-χ measurement for $B \parallel ab$.[9] The arrow indicates T_N of Eu^{2+} moments in the superconducting state in the absence of an applied field at 2.6 GPa.[9]

parameter λ_m used in the complete formula[12,34] is typically ignored for simplicity.[32,35] The Maki parameter α is defined as $\sqrt{2}\ B_{c2}^*/B_p$, using the orbital critical field B_{c2}^* at $T=0$ and the Pauli-Clogston paramagnetic limit B_p[36]. Reduced units—$t=T/T_c$, $h=0.281\ \ B_{c2}/B_{c2}^*$, and $h_J=0.281\ \ B_J/B_{c2}^*$—are employed. We assume $B_J=\beta\ \ M$ (β: constant), where the magnetization M is modeled within a molecular-field approximation.[37] To simplify the following discussions, α for $B \parallel ab$ is set to 3, a typical value for "122" systems.

The solid curve in Fig. 3 was calculated from Eq. (1) for B_{c2}^0 data with T_c set to the experimental value $T_c=29$ K. The fit yields a parameter set $(\lambda_{so},\ \beta)=(7.9,\ -187)$. $\beta=-187$ indicates that the maximum of $|B_J|$, B_J^m, is around 168 T. The fit captures the qualitative characteristics of the experimental B_{c2}^0 curve satisfactorily, especially the positive curvature below $T_N=20$ K, and shows that the low value of B_{c2} (compared to other Fe-based SCs' with similar T_c values) is due to the large B_J, which is a consequence of a large Eu^{2+} magnetization due to the field-induced FM alignment of the Eu^{2+} moments. However, its deviation from the experimental curve is also noticeable at low fields near T_c. This disagreement probably indicates that the phase diagram in this T-range is affected by a subtle competition between superconductivity and magnetic fluctuations, and it is beyond the scope of Eq. (1), which assumes a homogeneous B_J produced by paramagnetic spins. Since the dominant interaction among the Eu^{2+} moments is the intralayer FM interaction,[18,19,23,24] the FM fluctuations develop when T is lowered to T_N, as evidenced by the enhancement of the magnetic susceptibility as $T \rightarrow T_N$.[9,19,23] Such FM fluctuations may be detrimental to

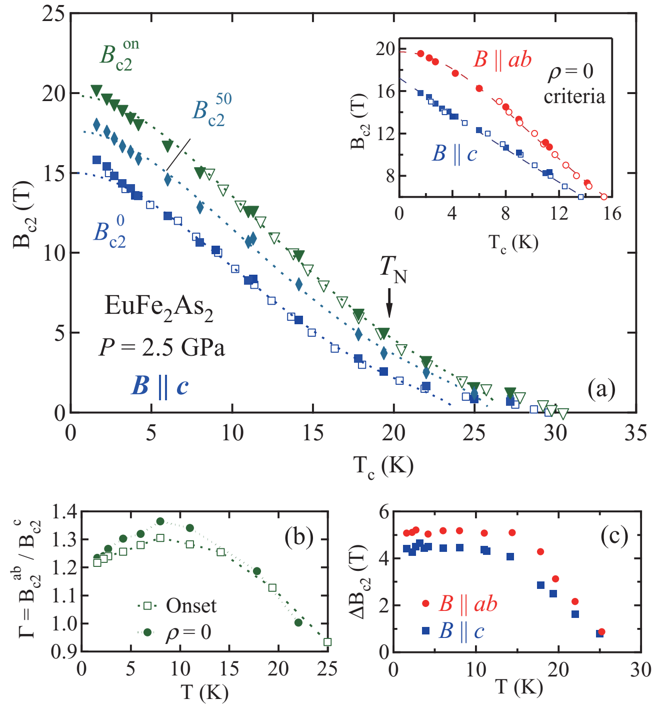

FIG. 4. (Color online) (a) $B_{c2}-T_c$ phase diagram of $EuFe_2As_2$ for $B \parallel c$ at 2.5 GPa. The solid and open symbols denote B_{c2} deduced from $\rho(H)$ and $\rho(T)$ data, respectively. The dashed curves are fits to Eq. (1). The inset shows B_{c2}^0 vs T_c for $B \parallel ab$ and $B \parallel c$. The dashed curves are fits for $T=0$ extrapolation (see text). (b) T variation of an anisotropy parameter, $\Gamma=B_{c2}^{ab}/B_{c2}^{c}$, determined by the onset and zero resistivity. (c) T dependence of the superconducting transition width, ΔB_{c2} $(=B_{c2}^{on}-B_{c2}^{0})$, for $B \parallel ab$ and $B \parallel c$.

superconductivity. One way to phenomenologically overcome this problem and to improve the fit in a T-range not close to T_c is to use a reduced value of T_c. Thus, the three dotted curves are calculated using the reduced T_c value. They reproduce the experimental curves excellently over the entire T-range, with a minimum temperature of 1.6 K. For B_{c2}^0, we assumed $(\lambda_{so},\ \beta,\ T_c)=(2.7,\ -83,\ 24\ \text{K})$, where $B_J^m \sim 75$ T. Here, it may be worthwhile to compare the parameters with those of the Chevrel compounds. The comparison revealed that he obtained λ_{so} is comparable to that found in the Chevrel-type Eu compounds,[32,35] and B_J^m in $EuFe_2As_2$ is a few times greater than that reported in the Chevrel-type Eu compounds.[32,35] We note that the concave curvature of B_{c2} in $EuFe_2As_2$ essentially differs from the positive curvatures often observed in highly two-dimensional SCs such as high-T_c cuprates. In the latter, the curvature is highly dependent on what criterion is chosen to define B_{c2}, and it is most likely affected by the vortex lattice phase transitions (i.e., from a vortex-liquid state to a vortex-solid state).[38]

Figure 4(a) shows the $B_{c2}-T_c$ phase diagram of $EuFe_2As_2$ for $B \parallel c$ at 2.5 GPa,[39] determined in the same manner as that used for B_{c2}^{ab}. A concave curvature around 20 K is also visible for the B_{c2}^c curves. The dashed curves are calculated using the parameters comparable to those used for B_{c2}^{ab}, that is, for B_{c2}^0, the fit gives $(\alpha,\ \lambda_{so})=(1.9,\ 2.6)$ when we assume

$(\beta, T_c) = (-83, 24\text{ K})$, identical to the values used for B_{c2}^{ab}. The calculated curves tend to saturate below 3 K, whereas the experimental curves appear to increase linearly as T decreases to zero. The unsaturation of B_{c2}^{c} has been observed in other Fe-based SCs,[14,40–42] and it has been explained using a two-band model. Figure 4(b) shows the anisotropy ratio, $\Gamma = B_{c2}^{ab} / B_{c2}^{c}$, calculated from $B_{c2}^{0}(T)$ and $B_{c2}^{on}(T)$. In spite of the quasi-two-dimensional layered structure in $EuFe_2As_2$, we obtain a small value of Γ, ranging between 0.9 and 1.4, which is comparable to that obtained for other "122" compounds.[40–43] In contrast to the monotonic decrease in Γ with decreasing T in other "122" compounds, Γ in $EuFe_2As_2$ exhibits a broad maximum at around 8 K, which is likely ascribed to the presence of the B_J.

In order to compare the magnitude of $B_{c2}(0)$ with that of other Fe-based SCs, we estimate it by extrapolating the low-T data to $T = 0$, as shown by the dashed curves in the inset of Fig. 4(a). For the extrapolations, an empirical expression, $B_{c2}(t) = B_{c2}(0)(1 - t^2)/(1 + t^2)$,[44] and a linear fit are used for B_{c2}^{ab} and B_{c2}^{c}, respectively. We obtain $B_{c2}^{ab}(0) = 24.7$ T and 19.7 T and $B_{c2}^{c}(0) = 21.5$ T and 17.2 T for B_{c2}^{on} and B_{c2}^{0}, respectively. $B_{c2}(0)$ in $EuFe_2As_2$ is significantly lower than $B_{c2}(0) > 50$ T in other Fe-based SCs at $T_c =$ 20–30 K.[14,40–42] The width of the superconducting transition, ΔB $(=B_{c2}^{on} - B_{c2}^{0})$, increases as T decreases to 15 K for both $B \parallel ab$ and $B \parallel c$ [Fig. 4(c)]. Below 15 K, ΔB is virtually T independent, as reflected by the parallel shifts of the $\rho(B)$ curves in Figs. 2(a) and 2(c). The T dependence may correlate with the development of M; M at $B = B_{c2}(T)$ increases rapidly as T decreases from T_c, but it is virtually saturated below ~15 K.[19] At 1.6 K, ΔB is estimated as 5.1 T and 4.4 T for $B \parallel ab$ and $B \parallel c$, respectively. The relatively narrow transition width at low-T, which is also observed in $Ba(Fe,Co)_2As_2$,[42,43] signifies a strong vortex pinning force in $EuFe_2As_2$.

In conclusion, we carried out high-field resistivity measurements up to 27 T for $EuFe_2As_2$ at 2.5 GPa, and we constructed the $B_{c2}-T_c$ phase diagram down to a minimum temperature of 1.6 K. Our analysis was based on a multiple pair-breaking model, and it revealed that the distinctive B_{c2} curves with positive curvature and the reduced B_{c2} values can be attributed to the substantial negative exchange field from the Eu^{2+} moments. The low temperature anisotropy at 1.6 K, $\Gamma = 1.2$, is comparable to the results obtained for other "122" systems.

[1] Y. Kamihara, T. Watanabe, M. Hirano, and H. Hosono, J. Am. Chem. Soc. **130**, 3296 (2008).
[2] For recent reviews, see K. Ishida, Y. Nakai, and H. Hosono, J. Phys. Soc. Jpn. **78**, 062001 (2009); D. C. Johnston, Advances in Physics **59**, 803 (2010).
[3] H. Kito, H. Eisaki, and A. Iyo, J. Phys. Soc. Jpn. **77**, 063707 (2008).
[4] Z.-A. Ren *et al.*, Chin. Phys. Lett. **25**, 2215 (2008).
[5] C. Wang *et al.*, Europhys. Lett. **83**, 67006 (2008).
[6] P. L. Alireza, J. Gillett, Y. T. Chris Ko, S. E. Sebastian, and G. G. Lonzarich, J. Phys. Condens. Matter **21**, 012208 (2009).
[7] Z. Ren *et al.*, Phys. Rev. Lett. **102**, 137002 (2009).
[8] K. Matsubayashi *et al.*, J. Phys. Soc. Jpn. **78**, 073706 (2009).
[9] T. Terashima *et al.*, J. Phys. Soc. Jpn. **78**, 083701 (2009); **78**, 118001 (2009); Physica C **470**, S443 (2010).
[10] W. Yu *et al.*, Phys. Rev. B **79**, 020511(R) (2009).
[11] T. Yamazaki *et al.*, Phys. Rev. B **81**, 224511 (2010).
[12] N. R. Werthamer, E. Helfand, and P. C. Hohenberg, Phys. Rev. **147**, 295 (1966).
[13] H. Kotegawa, H. Sugawara, and H. Tou, J. Phys. Soc. Jpn. **78**, 013709 (2009).
[14] F. Hunte *et al.*, Nature (London) **453**, 903 (2008).
[15] H. Raffius *et al.*, J. Phys. Chem. Solids **54**, 135 (1993).
[16] H. S. Jeevan *et al.*, Phys. Rev. B **78**, 052502 (2008).
[17] Z. Ren *et al.*, Phys. Rev. B **78**, 052501 (2008).
[18] Y. Xiao *et al.*, Phys. Rev. B **80**, 174424 (2009).
[19] S. Jiang *et al.*, N. J. Phys. **11**, 025007 (2009).
[20] C. F. Miclea *et al.*, Phys. Rev. B **79**, 212509 (2009).
[21] N. Kurita *et al.*, e-print arXiv:1008.0684 (to be published in J. Phys: Conf. Ser.).
[22] K. Matsubayashi *et al.*, e-print arXiv:1007.2889.
[23] T. Terashima *et al.*, J. Phys. Soc. Jpn. **79**, 103706 (2010).
[24] Y. Xiao *et al.*, Phys. Rev. B **81**, 220406(R) (2010).
[25] Y. Uwatoko *et al.*, Physica C **329-333**, 1658 (2003).
[26] K. Murata *et al.*, Rev. Sci. Instrum. **79**, 085101 (2008).
[27] R. H. Liu *et al.*, Phys. Rev. Lett. **101**, 087001 (2008).
[28] M. Gooch B. Lv, B. Lorenz, A. M. Guloy, and C. W. Chu, Phys. Rev. B **79**, 104504 (2009).
[29] N. Kurita *et al.* (unpublished).
[30] Ø. Fischer *et al.*, J. Phys. C **8**, L474 (1975).
[31] M. S. Torikachvili and M. B. Maple, Solid State Commun. **40**, 1 (1981).
[32] M. Decroux *et al.*, Phys. Rev. Lett. **52**, 1563 (1984).
[33] V. Jaccarino and M. Peter, Phys. Rev. Lett. **9**, 290 (1962).
[34] Ø. Fisher, Helv. Phys. Acta **45**, 331 (1972).
[35] C. Rossel *et al.*, J. Appl. Phys. **57**, 3099 (1985).
[36] B. S. Chandrasekhar, Appl. Phys. Lett. **1**, 7 (1962); A. M. Clogston, Phys. Rev. Lett. **9**, 266 (1962).
[37] The model reproduces experimental c-axis magnetization satisfactorily.[23] The anisotropy of magnetization is small, except for a low-T and low-B region;[19] hence, we use the same model for both $B \parallel ab$ and $B \parallel c$.
[38] Y. Ando *et al.*, Phys. Rev. B **60**, 12475 (1999).
[39] There is discrepancy between the present and previous B_{c2}^{c} data. The latter was determined from ac-χ.[9] This could be due to the difference in the applied pressure and/or sample variations. In this study, ρ was simultaneously measured using the two samples from the same piece.
[40] H. Q. Yuan *et al.*, Nature (London) **457**, 565 (2009).
[41] S. A. Baily *et al.*, Phys. Rev. Lett. **102**, 117004 (2009).
[42] M. Kano *et al.*, J. Phys. Soc. Jpn. **78**, 084719 (2009).
[43] A. Yamamoto *et al.*, Appl. Phys. Lett. **94**, 062511 (2009).
[44] A. Leitner, D. Olaya, C. T. Rogers, and J. C. Price, Phys. Rev. B **62**, 1408 (2000).